of this mechanism will certainly improve the description of the transition.

The author is grateful to Hansjörg Kaehr for his able technical assistance. He is much indebted to K. A. Müller for stimulating discussions, comments on the manuscript, and the communication of unpublished results. He has also benefitted from conversation with H. Thomas, T. Schneider, Th. von Waldkirch, and W. Berlinger, as well as from valuable suggestions of H. Gränicher and K. W. Blazey.

[1]*Structural Phase Transitions and Soft Modes*, edited by E. J. Samuelsen and J. Feder (Universitetsforlaget, Oslo, Norway, 1971).

[2]See Ref. 1 and references quoted therein.

[3]Th. von Waldkirch, K. A. Müller, W. Berlinger, and H. Thomas, Phys. Rev. Lett. 28, 503 (1972); Th. von Waldkirch, K. A. Müller, and W. Berlinger, Phys. Rev. B (to be published).

[4]K. A. Müller and W. Berlinger, Phys. Rev. Lett. 26, 13 (1971).

[5]K. A. Müller, W. Berlinger, M. Capizzi, and H. Gränicher, Solid State Commun. 8, 549 (1970). The author is very grateful to K. A. Müller and W. Berlinger for the loan of the sample used in Ref. 4. The curves reported here were obtained on the same crystal.

[6]This relation is experimentally known in other systems. See, for example, G. Egert, I. R. Jahn, and D. Renz, Solid State Commun. 9, 775 (1971).

[7]The effect of fluctuations on optical properties has been seen in the case of the paraelectric-ferroelectric transition. See, for example, R. Hofmann, Ph. D. thesis, Eidgenössische Technische Hochschule, 1968 (unpublished); M. G. Cohen, M. Di Domenico, Jr., and S. H. Wemple, Phys. Rev. B 1, 4334 (1970).

[8]M. Born and E. Wolf, *Principles of Optics* (Pergamon, New York, 1965), 3rd ed., p. 694. The author is indebted to Professor H. Gränicher for suggesting this compensator and for loaning an instrument at the beginning of the investigation.

[9]L. E. Cross and D. Chakravorty, in *Proceedings of the International Meeting on Ferroelectricity, Prague, Czechoslovakia, 1966*, edited by V. Dvořák *et al*. (Institute of Physics of the Czechoslovak Academy of Science, Prague, Czechoslovakia, 1966), p. 394.

[10]F. W. Lytle, J. Appl. Phys. 35, 2212 (1964).

[11]M. Born and E. Wolf, *Principles of Optics* (Pergamon, New York, 1965), 3rd ed., pp. 110–112.

[12]Detailed information will be published elsewhere.

[13]E. Pytte and J. Feder, Phys. Rev. 187, 1077 (1969); J. Feder and E. Pytte, Phys. Rev. B 1, 4803 (1970).

[14]J. Feder, in *Structural Phase Transitions and Soft Modes*, edited by E. J. Samuelsen and J. Feder (Universitetsforlaget, Oslo, Norway, 1971).

[15]Experimental data points communicated by K. A. Müller and W. Berlinger.

[16]J. C. Slonczewski and H. Thomas, Phys. Rev. B 1, 3599 (1970).

[17]K. A. Müller, private communication.

Two-Dimensional Character of the Conduction Bands of *d*-Band Perovskites*

T. Wolfram
North American Rockwell Science Center, Thousand Oaks, California 91360
(Received 14 August 1972)

The lowest conduction bands of a number of perovskites are determined principally by the $(pd\pi)$ interaction which mixes the t_{2g} d orbitals of the transition-metal ion with the p orbitals of the oxygen. Because of the planar character of the $(pd\pi)$ interaction, each of the three equivalent t_{2g} conduction bands depends strongly on only two of the conponents of the wave vector. As a result, the bands possess a two-dimensional character which accounts for the characteristic structure in the density of states and the optical properties of $SrTiO_3$, $BaTiO_3$, and $KTaO_3$.

The transition-metal perovskites such as $SrTiO_3$, $BaTiO_3$, and $KTaO_3$ have received considerable attention because of their many interesting electronic,[1-6] structural,[7-9] and optical[10-12] properties. Each of the above-mentioned materials is an ionic insulator with a band gap of 3 to 4 eV separating the d conduction band from the valence band. $BaTiO_3$ is ferroelectric[13] below the Curie temperature, and doped $SrTiO_3$ is a superconductor.[14] The photochromic and electrochromic properties of $SrTiO_3$ have been discussed recently,[15-19] and the electronic surface states of the d-band perovskites have also been studied by Wolfram, Kraut, and Morin.[20] Mattheiss has recently reported energy-band studies of these materials.[2]

The purpose of this Letter is to discuss a simple model which illustrates the two-dimensional nature of the lowest conduction bands. Analytical approximations are obtained for the energy bands

$E(k)$, density of states $N(E)$, joint density of states $J(E)$, and the frequency-dependent dielectric constant $\epsilon(\omega)$. The model $E(k)$ and $N(E)$ are in agreement with recent numerical calculations of Mattheiss.[2] The optical properties predicted yield an explanation of the low-energy reflectivity data of Cardona[10] for $SrTiO_3$ and $BaTiO_3$. Some important consequences of the two-dimensional energy bands are discussed.

The simplest linear-combination-of-atomic-orbitals (LCAO) model[21] for the transition-metal d-band ABO_3 perovskites utilizes fourteen orbitals: five d orbitals for the B transition-metal ion and nine p orbitals for the oxygens. Energy bands associated with the A ion are many electron volts above the lowest conduction bands and may be disregarded for the purposes of our discussion. The d bands are separated into the t_{2g} (lowest in energy) and the e_g bands because of the cubic crystalline field produced by the octahedron of oxygen surrounding the B ion. The oxygen anions experience an axial crystal field which splits the valence bands. In order of decreasing energy, the LCAO nearest-neighbor two-center transfer integrals[21] are $(pd\sigma)$, $(pd\pi)$, $(pp\sigma)$, and $(pp\pi)$. The oxygen-oxygen interactions are relatively weak. If they are neglected, our major points can easily be illustrated. This approximation yields qualitatively correct energy bands. The conduction bands are essentially unaffected by the approximation but it does produce some flat dispersion curves in the valence bands. The fourteen energy bands are given by

$$E_1 = E_\perp,\quad E_{\alpha\beta}^{(\pm)} = \tfrac{1}{2}(E_t + E_\perp) \pm r_{\alpha\beta};\quad E_2 = E_\parallel,\quad E_{xyz}^{(\pm\pm)} = \tfrac{1}{2}(E_e + E_\parallel) \pm s^{(\pm)};$$
$$r_{\alpha\beta} = \{[\tfrac{1}{2}(E_t - E_\perp)]^2 + 4(pd\pi)^2(S_\alpha^2 + S_\beta^2)\}^{1/2},\quad s^{(\pm)} = \{[\tfrac{1}{2}(E_e - E_\parallel)]^2 + 2(pd\sigma)^2[(S_x^2 + S_y^2 + S_z^2) \pm B^2]\}^{1/2}, \tag{1}$$
$$B^2 = (S_x^4 + S_y^4 + S_z^4 - S_x^2S_y^2 - S_x^2S_z^2 - S_y^2S_z^2)^{1/2},$$

where $\alpha\beta = xy$, xz, and yz; $S_\alpha = \sin k_\alpha a$; k_α are the components of the wave vector; a is the B-O bond distance; and $E_\perp$ and $E_\parallel$ are the diagonal p-orbital energies whose difference is due to the electrostatic splitting. Similarly, E_t and E_e are the diagonal energies of the t_{2g} and e_g d orbitals. E_1 is a threefold-degenerate valence band and E_2 is a nondegenerate valence band. $E_{\alpha\beta}^{(+)}$ gives three equivalent (t_{2g}-type) conduction bands and $E_{\alpha\beta}^{(-)}$ describes similar valence bands. $E_{xyz}^{(++)}$ and $E_{xyz}^{(+-)}$ are (e_g-type) conduction bands and $E_{xyz}^{(-+)}$ and $E_{xyz}^{(--)}$ are valence bands. The model described here is a simplification of that of Honig, Dimmock, and Kleiner[22] [see Eqs. (A15), (A16), (A18), and (A19) of Ref. 22]. In conventional notation, $E_\perp = E_{x_1,x_1}(000)$, $E_\parallel = E_{y_1,y_1}(000)$, $E_t = E_{xy,xy}(000)$, $E_e = E_{x^2-y^2,x^2-y^2}(000, pd\sigma) = E_{z^2,z^3}(00\tfrac{1}{2})$, and $(pd\pi) = E_{xy,y_1}(\tfrac{1}{2}00)$. The simple expressions in Eq. (1) for the conduction bands give an excellent representation of the bands determined by Mattheiss[2] for $SrTiO_3$, $KTaO_3$, $KMoO_3$, and ReO_3[23] and also of those determined by Kahn and Leyendecker[1] for $SrTiO_3$. The nature of the energy bands with and without the $(pp\sigma)$ and $(pp\pi)$ interactions are illustrated on the left-hand side of Fig. 1.

An essential point is that the t_{2g} conduction band described by $E_{\alpha\beta}^{(+)}$ depends only on two components of the wave vector.[24] As a result of this feature, the density of states possesses characteristic structure such as discontinuities at the band edges and a logarithmic singularity in the interior of the band. The model is suffi-

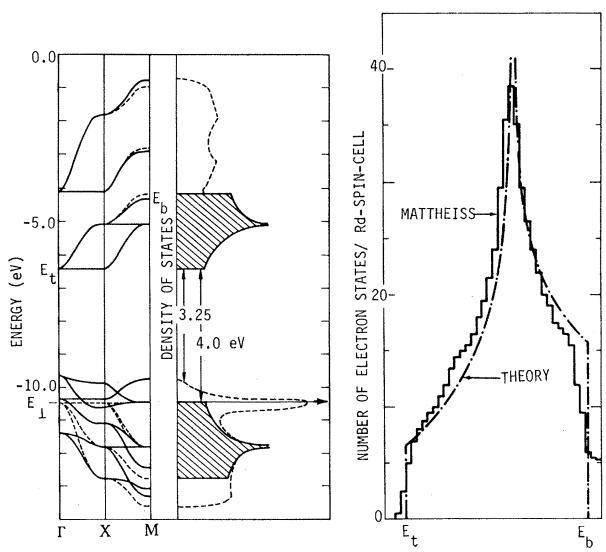

FIG. 1. Energy bands and density of states of $SrTiO_3$. The LCAO energy bands are indicated by the solid curves (left portion of the figure). The dashed curves are the energy bands neglecting $(pp\sigma)$ and $(pp\pi)$. The parameters used (in eV) are $E_\perp = E_\parallel = -10.43$, $E_t = -6.43$, $E_e = -4.1$, $(pd\sigma) = -2.23$, $(pd\pi) = 1.34$, $(pp\sigma) = 0.34$, and $(pp\pi) = -0.03$. The center figure is a schematic of the density of states. The shaded areas indicate the bands used in calculating $\epsilon_2(\omega)$. Right, the analytic density of states for the t_{2g} (lower) conduction band is compared with the numerical results of Mattheiss (Ref. 2). The upper edge $E_b = -4.41$ eV.

ciently simple that analytical results can be obtained for the single-particle Green's function $G(E)$:

$$G(E) = 2(\xi/\pi)\,|E - \tfrac{1}{2}(E_t + E_\perp)|\,K(\xi)/(pd\pi)^2,$$
$$\xi^2 = 4/(4-\zeta^2), \qquad (2)$$
$$\zeta = \tfrac{1}{2}[4(pd\pi)^2 - (E-E_t)(E-E_\perp)]/(pd\pi)^2,$$

where $K(\xi)$ is the complete elliptic integral with modulus ξ^2. Within the t_{2g} band, $\xi > 1$ and $K(\xi) = 1/\xi\{K(1/\xi) - i\,\mathrm{sgn}(\zeta)K((1-1/\xi^2)^{1/2})\}$.

The imaginary part of $G(E)$ is π times the density of states $N(E)$. A schematic of the density of states is shown in the center of Fig. 1. The shaded areas illustrate the theoretical density of states. The shaded portion of the valence- and conduction-band densities of states are mirror images of one another. On the right-hand side of Fig. 1, a quantative comparison is made with numerical calculations of the density of states obtained by Mattheiss[2] from a nineteen-parameter LCAO model which was fitted with his augmented-plane-wave (APW) calculations for $SrTiO_3$. The logarithmic character of the peak and the abrupt drop at the band edges are evident in the histogram. Similar results for the density of states are obtained for $BaTiO_3$, $KTaO_3$, and ReO_3. [The value of 1.34 eV used for $(pd\pi)$ in $SrTiO_3$ is somewhat larger than the "adjusted" value of 1.13 eV used by Mattheiss.[2] Soules *et al.*[3] and Kahn and Leyendecker[1] have reported values of 2.21 and 0.84 eV, respectively.]

The real part of $G(E)$ exhibits logarithmic singularities at the band edges and a discontinuity within the band.[25] *These two-dimensional characteristics are so dominant that they produce easily recognized structure in the dielectric function and hence in the optical properties.* In order to illustrate this, we consider the joint density of states $J(\omega) = \Omega^{-1}\int dK\,\delta(\omega - E_c + E_v)$, where Ω is the volume of the Brillouin zone, and E_c and E_v are the energies of the conduction and valence bands, respectively. The t_{2g} bands and the valence bands E_1, E_2, and $E_{\alpha\beta}^{(-)}$ determine the low-energy structure. A simple formula can be obtained for $J(E)$:

$$J(E) = 3N(E+E_\perp) + N(E+E_\parallel) + 3N[\tfrac{1}{2}(E+E_t+E_\perp)]. \qquad (3)$$

If the dipole matrix elements M_{vc} for transitions between the valence and conduction bands are approximately constant, then the imaginary part of the dielectric function $\epsilon_2(\omega)$ can be approximated by $\epsilon_2(\omega) = CJ(\omega)/\omega^2$, where C is a constant proportional to $|M_{vc}|^2$. The real part, $\epsilon_1(\omega)$, is obtained from the Kramers-Kronig relation,

$$\epsilon_1(\omega') - 1 = \int_{-\infty}^{\infty} d\omega\,\frac{\omega\epsilon_2(\omega)}{\omega^2 - \omega'^2} = \int \frac{d\omega\, C}{\omega^2 - \omega'^2}\,\frac{J(\omega)}{\omega} + \tilde{\epsilon}(\omega'), \qquad (4)$$

where $\tilde{\epsilon}$ accounts for other band contributions not included in $J(\omega)$. The situation is illustrated by the center portion of Fig. 1. The shaded regions are the bands included in the calculation of $J(\omega)$, while the dashed curves indicate the entire density of states. The arrow at $E_\perp = E_\parallel$ indicates the position of the flat bands used in the calculation of $J(\omega)$. Our objective here is not to produce an accurate calculation of $\epsilon(\omega)$, but rather to illustrate the structure that results from the two-dimensional nature of the bands. In Fig. 2, we illustrate this structure. The function ϵ_2 is calculated using Eq. (3) and choosing C so that the area under the peak from 4 to 5.6 eV agrees with experimental results[10] for $SrTiO_3$. A similar comparison is obtained for $BaTiO_3$. For simplic-

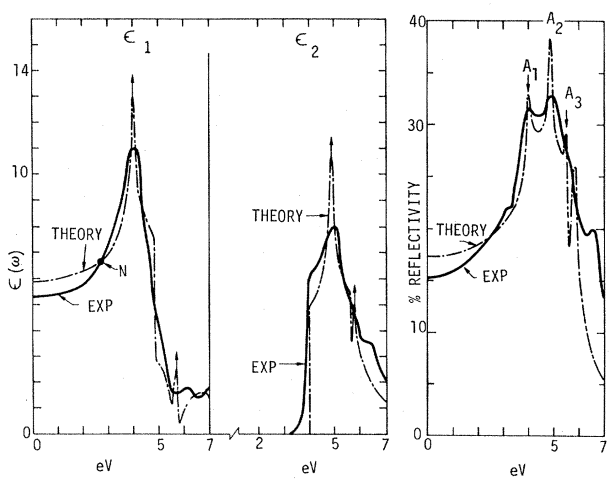

FIG. 2. Dielectric function and reflectivity of $SrTiO_3$. The theoretical functions $\epsilon_1(\omega)$ and $\epsilon_2(\omega)$ ($\hbar = 1$) are compared with experimental results (Ref. 10) on the left-hand side of the figure. The arrows indicate the positions of the logarithmic peaks. The theoretical reflectivity is compared with the experimental data of Cardona on the right-hand side of the figure. The logarithmic peaks have been made finite by averaging over a 0.01-eV interval, and a value of 1.03 eV is used for $(pd\pi)$, giving $E_B = -4.90$ eV.

ity, $\tilde{\epsilon}$ is taken to be a constant equal to 3.25. This normalizes ϵ_1 to Cardona's data at $\omega = 2.5$ eV.[10] These procedures are rather arbitrary, but the structure in ϵ is not dependent upon the particular method of normalization or the choice of C. The reflectivity R may be calculated from the relation $R = |(1-\sqrt{\epsilon})/(1+\sqrt{\epsilon})|^2$.

The calculated reflectivity is compared with the experimental data of Cardona in the right-hand side of Fig. 2 for $SrTiO_3$. The value of 1.03 eV used for $(pd\pi)$ is the same as the "fitted" value obtained by Mattheiss from his APW calculations.[2] The peaks at A_1 and A_2 as well as the shoulder at A_3 are in good agreement with the data. *The similarity between the theoretical and experimental curves strongly suggests that the essential features are determined by the two-dimensional character of the t_{2g} bands.*

The structure will be smeared out when the $(pp\sigma)$ and $(pp\pi)$ interactions are included. This effect also reduces the energy gap[11] to the observed 3.25 eV. Only slight structure will be produced at the fundamental absorption edge since the valence-band density is small at the band edge.

Several important points are implied by the model: (1) The peak in $N(E)$ arises from a *surface* in the Brillouin zone satisfying the equation $S_\alpha^2 + S_\beta^2 = 1$. The low-energy peak in ϵ_2 is produced by transitions to this surface from the valence band. While the points X in the Brillouin zone lie on this surface, the peaks in $N(E)$ and ϵ_2 cannot be attributed to these *point* contributions alone. (2) The doublet A_1 and A_2 in the reflectivity does not result from two different transitions, but rather from the peak in ϵ_2 and the peak in ϵ_1, and cannot be identified with any particular transition. For the two-dimensional density of states, one peak in ϵ_2 implies two peaks in the reflectivity. (3) If the density of electrons in the conduction band is expressed as $n = N_c \times \exp[-(E_t - E_F)/kT]$, where E_F is the Fermi energy, then because of the abrupt increases in $N(E)$ at the t_{2g} band edge, the effective density of states N_c increases linearly with temperature T rather than as $T^{3/2}$, characteristic of three-dimensional parabolic bands.[26] (4) Electronic impurity states will tend to be trapped in the energy gap because of the logarithmic singularities in $\mathrm{Re}(G)$ at the conduction-band edge.

The author wishes to express his appreciation to G. W. Lehman, W. F. Hall, F. J. Morin, and E. A. Kraut for helpful discussions, and to L. F. Mattheiss for making available preprints of his recent work on the perovskites.

---

*Work partially supported by the U. S. Air Force Office of Scientific Research under Contract No. F44620-72-C-0050.

[1]A. H. Kahn and A. J. Leyendecker, Phys. Rev. 135, A1321 (1964).

[2]L. F. Mattheiss, Phys. Rev. B 4, 3548 (1971).

[3]T. F. Soules, E. J. Kelley, D. M. Vaught, and J. W. Richardson, Phys. Rev. B 6, 1519 (1972); J. W. Richardson, E. J. Kelley, T. F. Soules, and D. M. Vaught, Bull. Amer. Phys. Soc. 16, 371 (1971).

[4]H. P. R. Frederikse, W. Therber, and W. R. Hosler, Phys. Rev. 134, A442 (1964), and Phys. Rev. 161, 822 (1967).

[5]Z. Sroubek, Phys. Rev. B 2, 3170 (1970).

[6]H. Yasunaga and I. Nakado, J. Phys. Soc. Jap. 22, 338 (1967), and 24, 218, 1035 (1968).

[7]J. M. Worlock and P. A. Fleury, Phys. Rev. Lett. 19, 1176 (1967).

[8]P. A. Fleury, J. F. Scott, and J. M. Worlock, Phys. Rev. Lett. 21, 116 (1968).

[9]G. Shirane and Y. Yamado, Phys. Rev. 177, 858 (1969).

[10]M. Cardona, Phys. Rev. 140, A651 (1965).

[11]K. W. Blazey, Phys. Rev. Lett. 27, 146 (1971).

[12]S. K. Kurtz, in *Proceedings of the International Meeting on Ferroelectricity, Prague, 1966,* edited by V. Dvorak, A. Fouskova, and P. Glogar (Institute of Physics, Czechoslovak Academy of Sciences, Prague, 1966), Vol. 1.

[13]A. Von Hippel, Rev. Mod. Phys. 22, 221 (1950).

[14]J. F. Schooley, W. R. Hosler, E. Ambler, J. H. Becker, M. L. Cohen, and O. S. Koonce, Phys. Rev. Lett. 14, 305 (1965).

[15]Z. J. Kiss, Phys. Today 23, No. 1, 42 (1970).

[16]B. W. Faughnan, D. L. Staebler, and A. J. Kiss, in *Applied Solid State Science,* edited by R. Wolfe, (Academic, New York, 1971), Vol. 2, pp. 107–172.

[17]B. W. Faughnan and Z. J. Kiss, IEEE J. Quantum Electron. 5, 17 (1969), and Phys. Rev. Lett. 21, 1331 (1968).

[18]B. Faughnan, Phys. Rev. B 4, 3623 (1971).

[19]J. Blanc and D. L. Staebler, Phys. Rev. B 4, 3548 (1971).

[20]T. Wolfram, E. A. Kraut, and F. J. Morin, to be published.

[21]J. C. Slater and G. F. Koster, Phys. Rev. 94, 1498 (1954); L. F. Mattheiss, Phys. Rev. 181, 987 (1969).

[22]J. M. Honig, J. O. Dimmock, and W. H. Kleiner, J. Chem. Phys. 50, 5232 (1969).

[23]L. F. Mattheiss, Phys. Rev. B 2, 3918 (1970).

[24]The dependence of the energy on only two components of the wave vector has been noted in Ref. 22, but the consequences were not investigated.

[25]The general character of singularities and discontinuities in the density of states has been discussed by L. Van Hove [Phys. Rev. 89, 1189 (1953)], and also by J. C. Phillips [Phys. Rev. 104, 1263 (1956)].

[26]The two-dimensional properties of the d bands of the

perovskites differ from those of graphite. Energy-band calculations based on a two-dimensional intralayer model yield a density of states which is continuous and increases linearly near the band edge. As a result, the real part of $G(E)$ does not have a logarithmic singularity at the band edge. However, when the interlayer interactions are added, the three-dimensional energy-band density of states rises discontinuously at the band edge. As a consequence, the effective number of electrons increases linearly with temperature. [See P. R. Wallace, Phys. Rev. 71, 662 (1947), and 72, 258 (1947), and also discussions in J. C. Phillips, *Covalent Bonding in Crystals, Molecules and Polymers* (Univ. of Chicago Press, Chicago, Ill., 1969), p. 125].

Observation of a Frequency Dependence in the Conduction-Electron Spin Resonance of Al, Cu, and Ag, Interpreted as a New Many-Body Effect in Metals with g Anisotropy*

D. Lubzens, M. R. Shanabarger,† and S. Schultz
University of California, San Diego, La Jolla, California 92037
(Received 24 October 1972)

The linewidth and g value for the conduction-electron spin-resonance-transmission line shape of aluminum was observed to be frequency and temperature dependent. The data are interpreted as a consequence of motional narrowing and many-body exchange in metals with g anisotropy, a many-body parameter for the spin part of the Landau correlation function, and the behavior of a relevant relaxation time.

We report our measurements of the frequency and temperature dependence of the conduction-electron spin resonance (CESR) line-shape parameters for Al, Cu, and Ag. We analyze our data in terms of a model which assumes appreciable g anisotropy over the Fermi surface and both motional narrowing and many-body exchange effects. The theoretical assumptions and equations used are discussed in detail in the following Letter by Fredkin and Freedman (FF). The experiments were performed utilizing the transmission technique (TESR)[1] on single-crystal samples at frequencies of 9.2 and 35 GHz, and over a temperature range from 1.3 to ≈ 50°K.

In Fig. 1 we present the Al CESR linewidth ($\Delta H = 1/\gamma T_2^*$) as a function of temperature for our two frequencies.[2] The data at 9.2 GHz are similar to those presented in the paper reporting the initial observation of CESR in Al.[3] The data at 35 GHz are markedly different from those at 9.2 GHz in several respects. The linewidth is also independent of temperature up to ≈ 20°K, but is considerably larger. At temperatures above 20°K the line *narrows* and then ultimately broadens again at still higher temperatures. For both Cu and Ag the phonon-dominated linewidth at high temperatures becomes independent of frequency,[4] but as can be seen from Fig. 1 for Al the data (note the log scale) suggest a constant high-temperature linewidth difference of ≈ 20 G. Since the data analysis we will present is consistent with the assumption that the extra 20 G develop at the higher temperatures, it is suggested that there may be a frequency dependence to the phonon-induced spin-flip scattering.

In Fig. 2 we present data for the observed CESR g value ($\bar{g}$) in both Cu and Al as a function of tem-

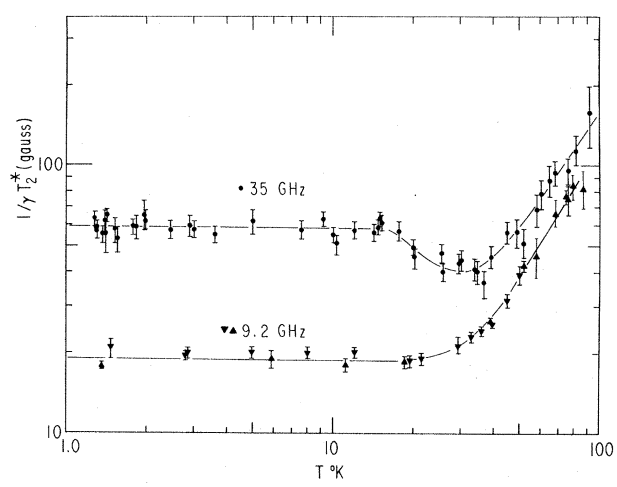

FIG. 1. Temperature dependence of the CESR linewidth $\Delta H = 1/\gamma T_2^*$, for single-crystal Al at 9.2 and 35 GHz. A typical sample was ≈ 0.004 cm thick and had a resistivity ratio [(room temperature)/4.2°K] ≈ 1600. In most cases the data at both frequencies were taken on the same sample. A similar frequency and temperature dependence was found for Cu and Ag except that, in contrast to Al, the linewidths were also a function of the orientation of both the magnetic field and the crystallographic axis, and the linewidth became independent of frequency at the higher temperatures (Ref. 4).